# Brain Magnetic Resonance Elastography based on Rayleigh damping material model

Andrii Petrov[1], Geoffrey J Chase[1], Mathieu Sellier[1], Peter Latta[2], Marco Gruwell[2], Matthiew McGarry[3] and Elijah Van Houten[4].

[1]Centre for Bioengineering, University of Canterbury, Christchurch, New Zealand; [2]Institute for Biodiagnostics, National Research Council of Canada, Winnipeg, Canada; [3]Thayer School of Engineering, Dartmouth College, Hanover, NH, United States; [4]University of Sherbrooke , Sherbrooke, Quebec, Canada

## Introduction

**Magnetic Resonance Elastography** (MRE) has demonstrated its ability to quantify soft tissue elasticity deduced from displacement measurements within the tissue obtained by phase-contrast Magnetic Resonance Imaging (MRI) techniques [1]. It is believed to have potential in the detection of wide variety of pathologies, diseases and cancer formations, especially tumors [2, 3].

Recently, Rayleigh, or *proportiona*l, damping (RD) moduli for soft tissue attenuation has been introduced to the non-linear, optimization based, subzone reconstruction method [4] to provide a more accurate model for the elastic energy attenuation occurring in the brain tissue under time-harmonic actuation. This research continues interest in the development of MRE methodologies for quantification of not only stiffness estimates, but also damping properties of the *in-vivo* brain.

## Background

### Rayleigh Damping Elastography

Rayleigh damping, also referred to as *proportional damping*, is a damping model that attributes attenuation to both elastic and inertial forces. Typically, the equilibrium statement for a damped elastic system is written as

$$\mathbf{M}\ddot{\mathbf{u}} + \mathbf{C}\dot{\mathbf{u}} + \mathbf{K}\mathbf{u} = \mathbf{f} \quad (1)$$

for displacements **u**, given forcing **f**, and a discretized stiffness matrix, **K**, mass matrix **M**, and damping matrix **C**. For a Rayleigh damped system, the damping matrix is directly proportional to the mass and stiffness matrices,

$$\mathbf{C} = \alpha\mathbf{M} + \beta\mathbf{K} \quad (2)$$

In time-harmonic steady state elastography, motion and force can be written as $\mathbf{u}(x,t) = \bar{\mathbf{u}}e^{i\omega t}$ and $\mathbf{f}(x,t) = \bar{\mathbf{f}}e^{i\omega t}$ thus giving:

$$(-\omega^2\mathbf{M} + i\omega\mathbf{C} + \mathbf{K})\bar{\mathbf{u}} = \bar{\mathbf{f}}. \quad (3)$$

where **K** and **M** are original undamped stiffness and mass matrices, respectively. Considering that the terms $(1 + i\omega\beta)$ and $(1 - i\alpha/\omega)$ carry the spatial information of Rayleigh damping parameters, the Eq (4) can be simplified as following:

$$\left[-\omega^2\mathbf{M}' + \mathbf{K}'\right]\bar{\mathbf{u}} = \bar{\mathbf{f}} \quad (4)$$

where **K**′ and **M**′ have the same form as the original stiffness and mass matrices, **K** and **M**, except for the use of a complex valued shear modulus, $\mu = \mu_R + i\mu_I$ and density $\rho = \rho_R + i\rho_I$ In this case, $\mu_R$ and $\rho_R$ represent the elastic shear modulus and mass density originally present in the undamped system, while the imaginary components can be written in terms of the Rayleigh damping parameters from Eq. 2 as

$$\rho_R = \rho,\ and \rho_I = \frac{-\alpha\rho}{\omega} \qquad \mu_R = \mu,\ and\ \mu_I = \omega\beta\mu.$$

From the damped elastic system model, described in Eq. 4, the damping ratio, can be written as

$$\xi_d = \frac{1}{2}\left(\frac{\mu_I}{\mu_R} - \frac{\rho_I}{\rho_R}\right). \quad (5)$$

which gives the relative level of attenuation within the material. For RD materials, an additional Rayleigh composition (RC) measure can be defined as

$$RC = \frac{-\mu_I}{2\mu_R\xi_d}, \quad (6)$$

RC value can be associated with the percentage contribution of viscoelastic effects to the overall damping profile of the material and can be approached through proportional rate of change of elastic vs. inertial forces argument.

## Materials & Methods

### Tissue simulating damping phantom studies

Three damping phantoms were manufactured to investigate performance of the reconstruction algorithm.

- D1 phantom ⟶ soft tofu background with a stiff 10% gelatin inclusion
- D2 phantom ⟶ stiff 10% gelatin background with a soft tofu inclusion.
- D3 phantom ⟶ firm / soft tofu background with a water inclusion

### *In-vivo* brain studies

*In-vivo* brain experiments were performed on a 3T Tim Trio Siemens MRI scanner using a standard single channel head coil. Vibrations were induced via two pressure actuated drivers (PADs), placed under the subject's head in the MRI head coil. Two active subwoofers, modified with airtight acrylic lids, were used to generate acoustic waves delivered through long tubing to the PADs [5].

## Results

### Tissue simulating damping phantoms results

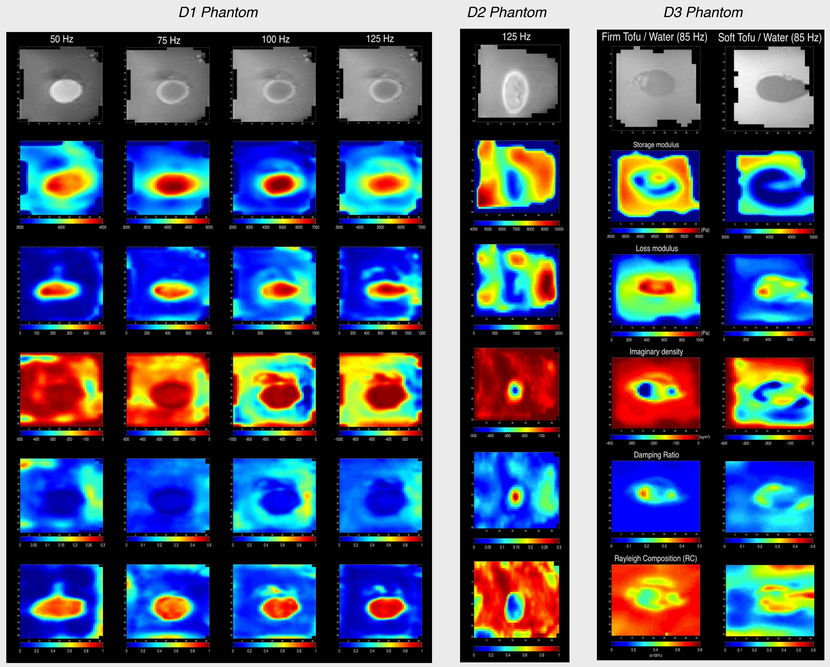


*ROI slice-by-slice analysis of reconstructed parameters (D1, 125 Hz)*

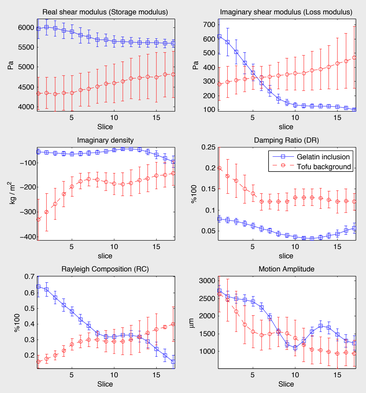


*ROI analysis of two in-vivo brain data sets (50 Hz)*

| RD | $\mu_R$ (Pa) | $\mu_I$ (Pa) | $\rho_I$ $(kg/m^2)$ | $\xi_d$ (%100) | $\xi_{CSM}$ (%100) |
|---|---|---|---|---|---|
| Ventricles | 843 ± 508 | 525 ± 403 | -514 ± 406 | 0.87 ± 0.51 | 0.47 ± 0.21 |
| White / Gray Matter | 2023 ± 730 | 967 ± 565 | -316 ± 347 | 0.51 ± 0.36 | 0.72 ± 0.24 |

| RD | $\mu_e$ (Pa) | $\mu_i$ (Pa) | $\rho_i$ $(kg/m^2)$ | $\xi_d$ (%100) | $\xi_{CSM}$ (%100) |
|---|---|---|---|---|---|
| Ventricles | 1070 ± 778 | 1095 ± 738 | -500 ± 427 | 1.07 ± 0.83 | 0.7 ± 0.25 |
| White / Gray Matter | 1992 ± 804 | 1150 ± 707 | -281 ± 378 | 0.52 ± 0.48 | 0.72 ± 0.25 |

### In-vivo healthy brain results

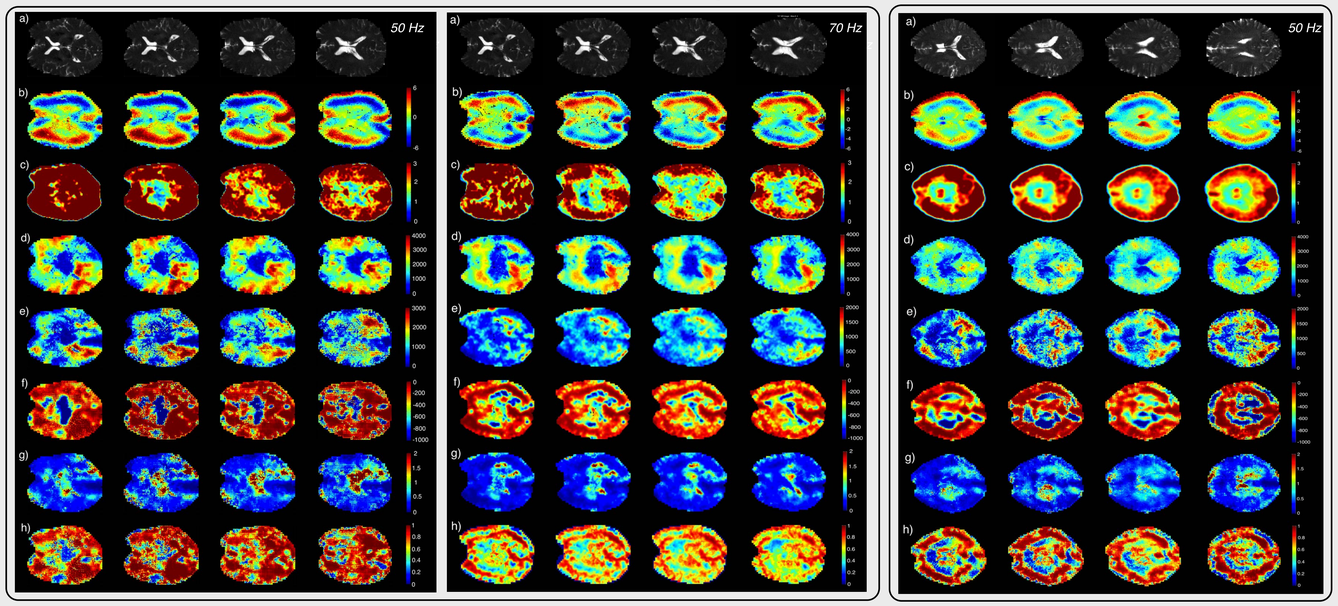


Rayleigh Damping (RD) MRE reconstruction results performed on a healthy human brain using 50 Hz and 70 Hz mechanical excitation: (a) T2-weighted MR image for anatomical reference; (b) real part of the displacement image; (c) OSS based SNR image [6]; (d) Storage modulus image (Pa); (e) Loss modulus image (Pa); (f) Imaginary density image (kg/m2), which for incompressible case represents fluid flow out of the elastic matrix; (g) Damping Ratio image, indicating a relative measure of the attenuation in the brain tissue; (h) Rayleigh Composition image, representing a relative measure of the damping mechanism in the brain tissue.

## Discussion & Conclusion

### Tissue simulating damping phantom studies

- RD model applied to MRE is able to accurately measure viscoelastic properties, damping behavior and elastic energy attenuation mechanism of the tissue simulating damping phantoms.
- The reconstructed parameters have shown a good correlation with the geometrical dimensions of the physical structures of both phantoms.
- Qualitatively, DR was reconstructed correctly for both materials across multiple frequencies. In the D2 the magnitude of the DR is increasing in the vicinity of tofu inclusion correctly confirming higher loss of mechanical energy in the more highly attenuating tofu material compared to the stiffer gelatin background. On the other hand, the gelatin inclusion in the D1 phantom has a lower damping than the tofu background correctly describing damping characteristics of both materials.
- Qualitatively, the RC reconstructions of the D1 phantom clearly distinguish the location of the gelatin inclusion within the tofu background across multiple frequencies. In the D2 phantom, the presence of the tofu inclusion is clearly depicted in low RC values, while stiffer gelatin background is reconstructed in the high RC values.
- The results observed in both phantom configurations seem to indicate that the high RC values correspond to the tightly grouped, randomly arranged collagen strands of gelatin while low RC values match fluid saturated structure of tofu.

### *In-vivo* healthy brain studies

The first results achieved by the RD brain MRE show promise for potential *in-vivo* determination of different brain tissue types, and the possibility of providing additional diagnostic tools. Moreover, the values obtained for brain viscoelastic properties agree well with *in-vitro* and *in-vivo* brain data published elsewhere [7,8]. Further RD brain elastogrpahy experiments as well as studies of a variety brain simulating damping phantoms are needed to investigate attenuation mechanisms across different intracranial tissue types, including tissue in diseased states such as multiple sclerosis, Alzhiemer's, hydrocephalus and cancer.

## References

**1.** R. Muthupillai, D. J. Lomas, P. J, Rossman, J. F. Greenleaf, A. Manduca, R. L. Ehman, Magnetic resonance elastography by direct visualization of acoustic strain waves. Science, vol. 269, pp. 1854–1857, 1995.

**2.** Xu L, Lin J, Han JC, Shen H, Gao PY, Magnetic resonance elastography of brain tumors: preliminary results. Acta Radiol, vol. 48, no. 3, pp. 327–330, 2007

**3.** Wuerfel, F. Paul, B. Beierbach, U. Hamhaber, D. Klatt, S. Papazoglou, F. Zipp, P. Martus, J. Braun, and I. Sack, MR-elastography reveals degradation of tissue integrity in multiple sclerosis, Neuroimage, vol. 49, no. 3, pp. 2520–2525, Feb 2010.

**4.** Van Houten, EEW., et al., Subzone based magnetic resonance elastography using a Rayleigh damped material model, Medical Physics, vol. 38, 2011

**5.** Latta, P., et al., Convertible pneumatic actuator for magnetic resonance elastography of the brain. Magnetic Resonance Imaging, vol. 1, pp. 147-152, 2010

**6.** McGarry, MDJ., et al., An octahedral shear strain-based measure of SNR for 3D MR elastography, Physics in Medicine and Biology, vol. 56, no. 13, N153, 2011

**7.** M. A. Green, L. E. Bilston, and R. Sinkus, In vivo brain viscoelastic properties measured by magnetic resonance elastography, NMR in Biomedicine, vol. 21, no. 7, pp. 755–764, 2008.

**8.** J. Zhang, M. Green, R. Sinkus, and L. Bilston, Viscoelastic properties of human cerebellum using magnetic resonance elastography, Journal of biomechanics, vol. 44, no.10, pp. 1909–1913, 2011.